Charles University

Faculty of Science

Study programme: Chemistry

Branch of study: Chemistry

Mária Piatková

Polymeric framework materials as a noble metal free heterogeneous catalyst

Polymerní síťované struktury jako heterogenní katalyzátory neobsahující ušlechtilé kovy

Bachelor´s thesis

Supervisor: Dr. Michael Janus Bojdys

Prague, 2018

Prohlašuji, že jsem tuto bakalářskou práci vypracovala samostatně pod vedením školitele Dr. Michaela Janus Bojdyse, a že jsem uvedla všechny použité informační zdroje a literaturu. Tato práce ani její část nebyla použita k získání jiného, nebo stejného akademického titulu.

V……. dne …….. Mária Piatková

I declare, that I carried out this bachelor´s thesis independently under the supervision of Dr. Michael Janus Bojdys, and that I cited all the sources properly. This thesis or its´ part was not used for getting another, or the same academic title.

In……. date …….. Mária Piatková

Acknowledgements

I would like to express my gratitude to my supervisor Dr. Michael Janus Bojdys for the opportunity to become a part of his group, for his guidance and his time. I would like to thank Dr. Dana Schwarz and Ing. Yaroslav Kochergin for their guidance and patience in the laboratory and for showing me my way around the synthetic laboratory. Further, I would like to say thank you to the whole group of functional materials. My gratitude also goes toward the Department of Organic Chemistry at the Faculty of Natural Sciences, Charles University and Institute of Organic Chemistry and Biochemistry of Czech Academy of Sciences were the experiments were performed. I want to thank the European Research Council for financial support. Lastly, my thanks belong to my family and friends for their continuous support.

Abstract

A functional triazine-based polymer framework with embedded copper (Cu) nanoparticles (Cu@TzP) is obtained from a one-pot, "wet" chemistry process that is easily scaled up to industrial demand. The polymer framework has permanent, guest-accessible microporosity and can be obtained as a membrane with 124 m^2g^{-1}, or as a bulk powder with 660 m^2g^{-1} (by Ar sorption). The Cu nanoparticles are generated *in situ* during the formation process of the polymer framework, and they serve as ideal, heterogenised active sites for C-N bond formation and enzyme-mimetic peroxidase catalysis. Further, we tune the porosity of the polymeric support matrix by thermal tempering (carbonisation). It turns out, that Cu@TzP performs best as a peroxidase-mimic in the form of a thin, accessible flake with 2 nm-sized Cu nanoparticles (NPs). Although no records were broken in terms of catalytic activity, we establish an attractive design principle of a scalable membrane support for noble-metal free catalysis.

Abstrakt

Funkční polymerní struktury obsahující triazinové motivy s včleněnými nanočásticemi mědi (Cu@TzP) je získána pomocí „mokrého“ chemického procesu odehrávajícího se v jedné baňce a který je jednoduše použitelný i pro větší industriální aplikace. Polymerní struktura má stálou, dostupní mikro porositu a může být získána jako membrána s povrchem 124 m^2g^{-1}, anebo jako prášek s povrchem 660 m^2g^{-1} (určeno pomocí Ar sorpce). Měděné nanočástice jsou generovány *in situ* v procesu formace polymerní struktury a slouží jako ideální, heterogenní aktivní místo pro tvorbu vazeb C-N a enzymovou imitaci peroxidázy. Dále, upravíme velikost povrchu polymerní struktury pomocí termálního zahřívání (karbonizace). Ukázalo se, že Cu@TzP dosahuje nejlepší výsledky jako peroxidázový materiál ve formě tenkých, dostupných membrán s měděnými nanočásticemi velikosti 2 nm. I když náš výzkum nepřelomil žádný rekord v oblasti katalýzy, připravili jsem zajímavý princip pro škálovatelnou přípravu membránového nosiče pro katalýzu bez použití ušlechtilých kovů.

Table of content

1. Introduction

Every day, thousands of industrially important products are made thanks to a use of catalysts. Catalyst have a huge effect on production cost, as the reaction occurs faster and requires less energy, for example in the form of heating or higher pressure. Furthermore, the catalysed reactions usually yield fewer side products and require less reagents due to higher conversion. These concepts are summarised in the 12 principles of green chemistry,[1] developed by Paul Anastas and John Warner to outline what makes a chemical process or product more environmental friendly, one of which is the use of efficient catalyst. One of the commonly catalytically synthetized structural motifs is the aromatic carbon-nitrogen bond. This motif is important in a wide range of scientific and industrial areas, such as pharmacology,[2] where it is an integral part of drug design, agriculture,[3] in which it is used for crop protection, and materials science,[4] more specifically they are used for example as a hole-transport layer in electroluminescence devices.[5] Therefore, a lot of synthetic approaches toward preparation of arylamines have been reported so far, most commonly, using palladium-catalysed C-N coupling.[6] The main drawback of this synthetic route, however, is high production cost and difficult recyclability of the noble metal catalyst, and hence other ways of arylamines synthesis, such as copper-based catalysis using boronic acids or aryl halides,[7] have been investigated. There are also reports on using copper nanoparticles (CuNPs) for synthesis of arylamines.[8] In organic synthesis the use of metallic nanoparticles is found to be often more effective than a bulk metal due to higher concentration of active sites and larger catalytically active surface area.

Recently, our laboratory has reported an insoluble membrane, which contains copper nanoparticles.[9] The polymerisation is done on copper foil and copper nanoparticles are formed as the polymer grows. This polymer embedded nanoparticles hold the potential for a catalytic activity of this material as a heterogeneous catalyst. Heterogeneous catalysts possess advantages compared to homogeneous, as they are easier to separate and therefore reuse.

Metals are also an important part of enzymes, including copper in a lot of examples,[10] which act as catalysts in living organisms. Compared to synthetically prepared catalysts, they are more effective and selective, but also hard to purify and usually exhibit low stability. That is what led people to exploring artificial enzymes, those are synthetic materials, which mimic the characteristics of enzymes, and they often contain metals in their active site.[11] In many cases copper proved itself useful in these applications[12]. One of such cases is an artificial peroxidase, an enzyme, which catalyses the oxidation of hydrogen peroxide and alkyl peroxides, and which found many uses,[13] mostly in sensing. Recently scientists used covalent triazine framework modified with Cu^{2+} as a peroxidase-like material[14]. Our catalytic system also contains triazine units and Cu in the form of nanoparticles, therefore we tested this polymeric membrane as an artificial peroxidase.

Our results show, that Cu@TzP shows only a moderate activity as a peroxidase-mimic and performs at its best in a membrane-like morphology with 2 nm CuNPs. Here, the open, sheet-like structure facilitates the accessibility of CuNPs by a very polar reaction medium. Conversely, C-N bond formation in less polar solvents – albeit sluggish - benefits from the

enhanced surface area of Cu@TzP conferred by carbonization. Although the catalytic performance of Cu@TzP is outmatched by heterogeneous noble-metal catalysts and some artificial enzymes, we believe that this study offers an important insight into the intrinsic catalytic activity of Cu@TzP; a material that has the clear benefit over its competitors that it can (a) be grown as a coating or membrane and (b) it can be obtained in a one-pot reaction.

2. Catalysis

A catalyst accelerates a chemical reaction by lowering the activation energy (E_a) of a reaction. Furthermore, catalysts are unchanged by chemical reaction. Every chemical reaction has its activation energy, a barrier separating two minima of potential energy. For a reaction to occur the reactant´s translational energy must be equal to or greater than the activation energy of a reaction. In presence of a catalyst the activation energy of reaction is lower, because the reaction occurs along a different pathway, as shown on the *Figure 1*, therefore more molecules have enough energy to undergo a chemical reaction, increasing the rate of the reaction. This principle is illustrated on *Figure 1*, where X, Y symbolizes the energy level of reactants and Z is the energy level of a product of a reaction. The highest point on the reaction profile corresponds to the energy of transition state and the difference between the energy of reactants and energy of transition state is activation energy. As can be seen from the reaction profile on *Figure 1* the catalyst decreases the activation energy. The difference between the energy of reactants and the energy of product is called Gibbs free energy (ΔG) and the value of Gibbs free energy is not affected using catalyst.

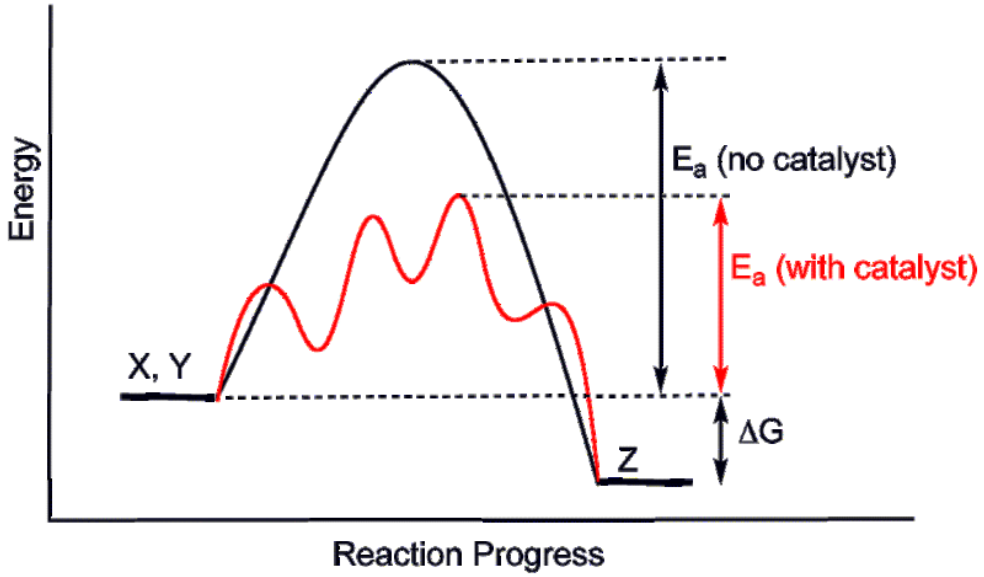

Figure 1. Reaction profile with and without a catalyst (source: Wikimedia commons)

The catalyst can be either in the same phase as the substrate, in which case we call it homogenous catalysis, or it can be in different phase than the substrate, then we talk about heterogeneous catalysis. Heterogeneous catalysis, unlike homogenous catalysis, provides easy catalyst separation and potential reusability of a catalyst, as catalyst is not changed or consumed by reaction, ideally, we could use the same catalyst forever. However, in case of homogenous catalysis it is often not possible to separate the catalyst after the reaction, or the separation is more expensive than producing a new catalyst. Even though the heterogeneous catalysts cannot be used forever in reality, due to side reactions, or non-full recovery of a catalyst the option of easily and non-expensively reusing them for a few times is an advantage compared to homogenous catalysts. During a catalysed reaction, the reactant usually forms an

intermediate with the catalyst which is further transformed to the product. The reaction of reactant with a catalyst is usually the rate determining step. In the heterogeneous catalysis this process is usually controlled by the adsorption on the solid surface.

2.1. Catalysing the C-N bond formation

Traditional approach to synthesis of C-N bond includes Buchwald-Hartwig coupling, which uses Pd catalyst[15].

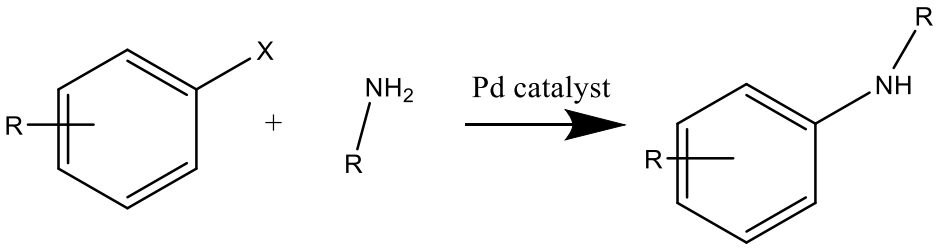

Scheme 1. General scheme of Buchwald-Hartwig reaction

This reaction can provide a very high yield of product. Butcher et al.[6a] used a palladium complexes of 2-formylpyridine thiosemicarbazone for a Buchwald-Hartwig reaction with yields up to 100% after more than 9 hours. Chen et al.[16] reports good to excellent yields for reaction of chlorobenzene with primary or secondary amines in presence of Pd complexes. Hajipour[17] reported yields of 100% after just 50 minutes when using palladium complex to catalyse Buchwald-Hartwig reaction with secondary amines. However, Pd as a noble metal is not the best substance for catalysis, further those catalysts are homogenous, which means they are not being reused. Therefore, researchers explored other ways for catalysing the formation of aromatic carbon nitrogen bond with the use of copper-based catalysts in Chan-Lam coupling reaction or Ullman reaction.

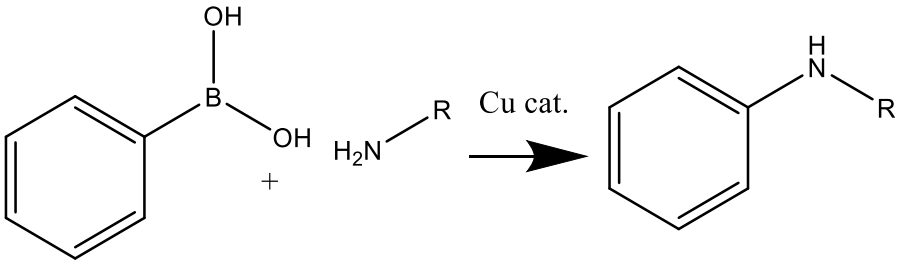

Scheme 2. General scheme for Chan-Lam reaction

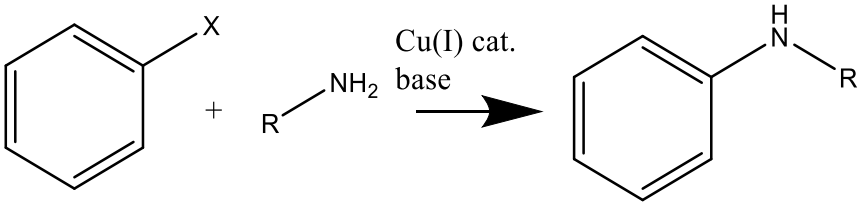

Scheme 3. General scheme for Ullman reaction

Variety of copper complexes has been reported for those reactions[7e, 18] and further, scientists explored using copper in other form than complexes for a catalyst in those reactions. Islam et al.[7c] have incorporated copper into a polymer network, which created reusable catalyst for C-N and C-O bond formation with yields up to 98%. There are also reported smaller molecules, such as copper oxide nanoparticles[8b] or copper nanoparticles[8a], to catalyse the C-N bond formation. In our study we focused on the Ullman reaction, which we tried to catalyse with the use of CuNPs embedded in the polymeric framework.

3. Peroxidase-like activity

3.1. *Artificial enzymes*

Enzymes are a special class of catalyst, which are found in living organisms. They are much more selective, and they usually exhibit better catalytic activity than man-made catalysts. To investigate the enzyme kinetics Michaelis and Menten[19] proposed a general mechanism for enzymatic reactions, in which substrate first reversibly binds to enzyme and then the enzyme catalyses chemical reaction and releases the product.

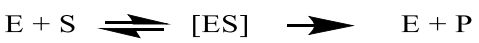

Figure 2. General mechanism of enzymatic reaction

This scheme leads to a well-known formula for the rate of enzymatic reaction:

$$v = \frac{V_{\mathrm{MAX}}[\mathrm{S}]}{K_{\mathrm{M}} + [\mathrm{S}]} \tag{1}$$

in which $[\mathrm{S}]$ is the concentration of a substrate, V_{MAX} is the maximum rate of a reaction and K_{M} is Michaelis-Menten constant. Michaelis-Menten constant is the substrate concentration required to reach half of V_{MAX}, this value is specific for each enzyme and substrate. K_{M} is a useful information for comparing the effectiveness of enzymes, the smaller the value of K_{M} the higher binding affinity the enzyme and substrate have. To determine those values, we can plot a dependence of rate of reaction over a concentration of a substrate, or we can use Lineweaver-Burke´s linearization of this equation. In this case we plot reciprocal value of rate of a reaction over a reciprocal value of substrate concentration, then we can determine the V_{MAX} and K_{M} from this graph as is shown on a *Figure 3*.

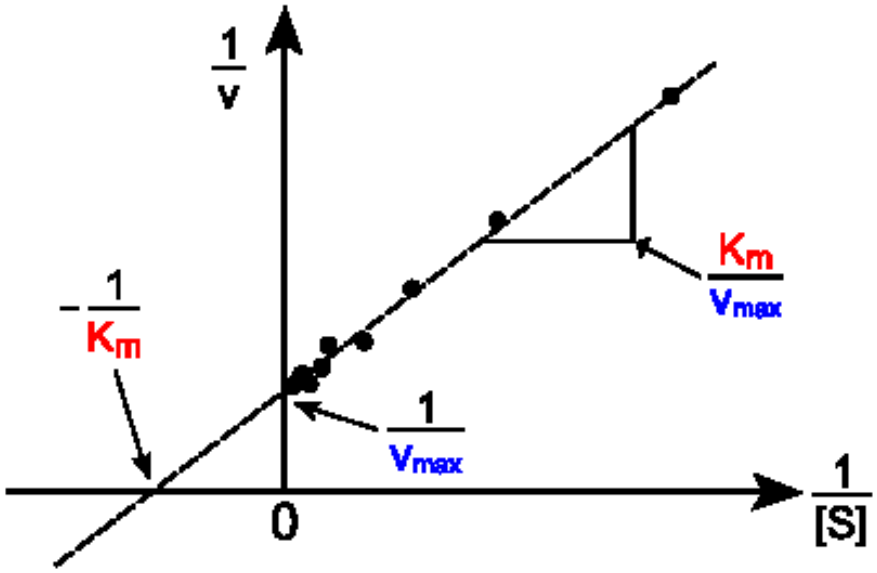

Figure 3. The Lineweaver-Burke plot of enzyme kinetics (source: Wikimedia commons)

Thanks to the high efficiency enzymes have found their use in various aspects of our lives,[20] couple of examples include enzymes in detergents for specific stain removals, lot of enzymes are used in food industry to firm the fruit products or to produce lactose-free milk, peroxidases are used as an antimicrobial agents and there are many more examples. Often thought the production cost, purification or durability of enzymes limit their use. This is what led scientists to the development of artificial enzymes, with one of the highly studied being artificial peroxidases.

3.2.Peroxidase mimetics

Peroxidases form a class of enzymes, which catalyse the oxidation of hydrogen peroxide and alkyl peroxides. These enzymes are used as biosensors,[13a] in diagnostics and histology.[13b, 13c] Naturally occurring peroxidases usually contain Fe, Mn or V in their active site. The most studied horseradish peroxidase contains haem-iron[21]. Due to the problems with the purification and stability of naturally occurring peroxidases the development of more stable, low-cost peroxidase is being done. Wei et al. reported intrinsic peroxidase properties of iron oxide,[22] what they used in H_2O_2 and glucose detection. Cheng et al. explored combination of artificial enzyme with a natural enzyme[13c] in monitoring brains of living organisms. Group of Fanggui Ye recently showed that Prussian blue nanoparticles[23] and Cu^{2+} containing triazine network[14] exhibit intrinsic peroxidase properties, which can be used in a variety of applications. The active site in the latter is Cu^{2+} atom and we aimed to explore if the Cu NPs in a polymeric membrane formed by triazine-based monomers can also exhibit peroxidase-like activity. Peroxidase can catalyse oxidation of tetramethylbenzidine (TMB), which when oxidised turns into a blue complex, therefore we can study this reaction by measuring the absorbance of light with wavelength 652 nm. Using the Lambeert-Beers law we can calculate the concentration and therefore determine the rate of reaction.

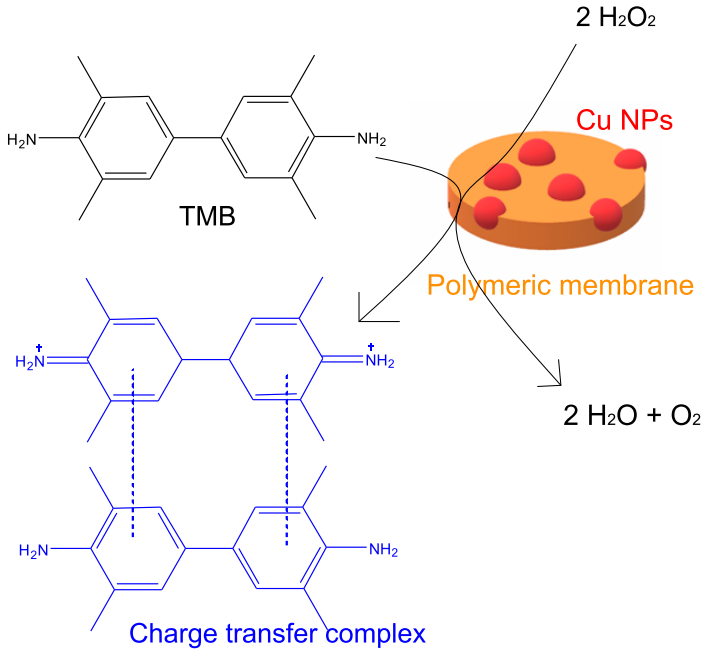

Figure 4. Schematic representation of tetramethylbenzidine oxidation by H_2O_2 with a polymeric membrane containing Cu nanoparticles acting as an artificial enzyme

4. Synthesis

Polymers were prepared in two ways. Firstly, we prepared polymer on a copper foil, which acted as a template and a catalyst. Then for comparison we prepared polymer in solution by traditional Glaser coupling reaction.

4.1. Preparation on copper plates

The polymerisation of 2,4,6-tris(4-ethynylphenyl)-1,3,5-triazine is done on copper foil in pyridine as a solvent. Copper foil acts as a 2D template as well as a catalyst. The expected product was 3D triazine-based graphdiyne formed by Glaser-type coupling of acetylenes. The obtained polymer consists of 2D/3D Van der Waals (VdW) heterostructure, 2D phase being formed by [2+2+2] cyclotrimerization resulting in a crystalline covalent triazine-based framework (TzF) and 3D triazine-based graphdiyne, formed by Glaser type coupling. The proposed mechanism suggests, that high concentration of surface-adsorbed monomers allows for [2+2+2] cyclotrimerization. In addition, a 2D template helps the formation of thermodynamically more stable 2D TzF. In the early stages of reaction nascent Cu NPs are formed. Further, they act as a catalytic site for Glaser-type coupling, resulting in 3D amorphous TzG.[9]

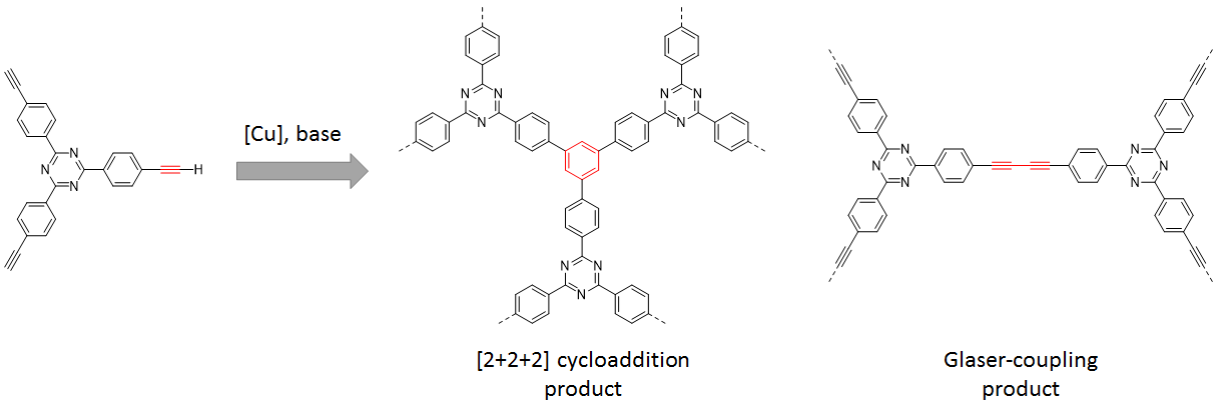

Figure 5. The reaction scheme of 2,4,6-tris(4-ethynylphenyl)-1,3,5-triazine polymerisation yielding [2+2+2] cycloaddition product and Glaser coupling product.

The [2+2+2] cyclotrimerisation of terminal alkynes was shown to occur on gold and silver surfaces, but under ultra-high vacuum conditions[24]. However, [2+2+2] cyclotrimerisation was not shown on copper surface before, under ultra-high vacuum the reaction proceeded in a mix of pathways without the preferred one[25]. Our material was prepared in a solution what eliminates problems, that can emerge when working under ultra-high vacuum. Material prepared under ultra-high vacuum will cover the surface and therefore can only be used for direct surface coverage, whereas our material can be easily etched from the copper foil to yield self-standing flakes.

4.2. Preparation in bulk

The material in bulk was prepared by a Glaser coupling, which was first described by Carl Glaser.[26] Glaser coupling is a homocoupling of terminal alkynes in presence of Cu(I) catalyst, its general scheme is on *Figure* ***6***.

Therefore, when preparing the material in bulk the only formed product is 3D triazine-based graphdiyne in the form of orange powder, which contained the Cu(I) salt.

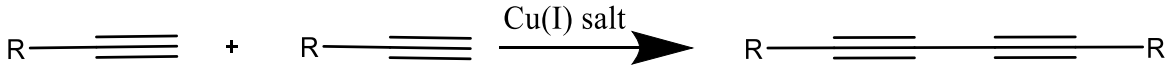

Figure 6 General scheme of Glaser coupling

4.3.Carbonisation

Prepared materials were carbonised in tubular furnace. Carbonisation is a process of heating the material up to a point at which it starts to change the structure. Parts of the material are being burnt away, creating pores in the structure, resulting in higher surface area. The carbonisation was done under inert atmosphere to prevent full oxidisation of the structure. The resulting carbonised material will contain structural subsets of the structural motifs of the original (i.e. a high nitrogen content and embedded CuNPs), but will now also feature larger transport channels, that might facilitate access to catalytically active sites.

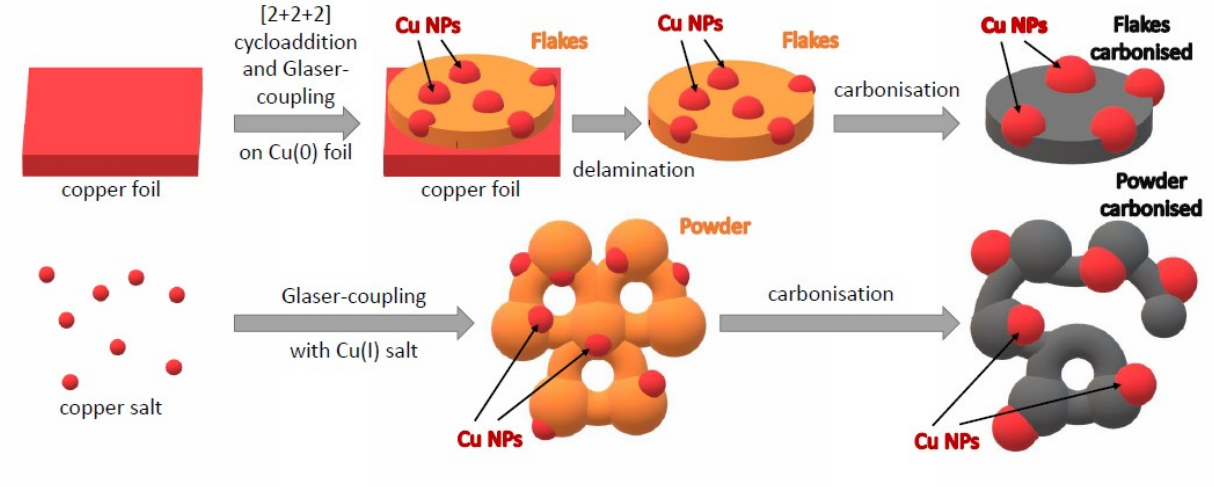

Figure 7. Schematic representation of synthesis of polymers on copper foil and in bulk using Cu(I) salt resulting in polymer membrane and powder respectively both with embedded CuNPs, and the process of carbonisation resulting in more porous polymers

5. Experimental section

5.1 Preparation of polymer

Scheme 4. Scheme of polymer synthesis

For the deprotection reaction 2,4,6-tris(4-((trimethylsilyl)ethynyl)phenyl)-1,3,5-triazine and potassium carbonate in molar ratio 1.6 was used. Both were put into the flask, anhydrous methanol and anhydrous THF in ratio 7.4 were added. Reaction ran under argon atmosphere overnight. The product was extracted with DCM and washed with brine solution. Organic phase was dried using magnesium sulphate and the solvent was removed *in vacuo*. The product was obtained as a light green solid.

Obtained monomer was then polymerised either on copper foil or in bulk.

5.1.1 Polymerisation on copper foil

First copper foil was washed with 1 M HCl, acetone and methanol. Cleaned foil was put into a three-neck flask, which was evacuated to dry the foil and then filled with argon. Pyridine was added to the flask. 50 mg of monomer dissolved in the pyridine were poured into the dropping funnel. The flask was heated up to 60°C and then the solution of monomer was slowly added. Reaction then ran for 4 days. After the pyridine was poured out, the copper foil was washed with warm acetone, DMF and acetone again. Afterwards the plates were dried over the vacuum. The polymer was taken off the copper plates using 1 M H_3PO_4 and a lot of water. The polymer was washed with 2 L of distilled water and dried in the oven overnight. The product was obtained as orange flakes.

5.1.2. Polymerisation in bulk

Flask with 0.25 g of monomer and 0.63 mmol of CuCl was filled with argon. 50 mL of pyridine were added, and the reaction mixture was heated up to 60°C. Reaction ran for 6 days. After completion of reaction the solid product was put into a Soxhlet thimble and washed with DMF, THF, Chloroform, water and methanol. Afterwards it was soxhleted with methanol and THF, both for one day. Product was dried in the vacuum oven and obtained as an orange powder.

Prepared polymers were carbonised under nitrogen atmosphere at 600°C or 800°C for 2 hours, with the rate of 5 K/min.

5.2. Procedure for preparation of diphenyl Amines

Scheme 5. General scheme for synthesis of arylamines

A stoichiometric amount of copper embedded in polymer, K_2CO_3, aniline and iodobenzene were combined in a flask in molar ratio 1.5 :1.2: 1 together with solvent. Reaction was done under the argon atmosphere. Conversion of the reaction was determined using HPLC.

5.3. General procedure for peroxidase activity testing

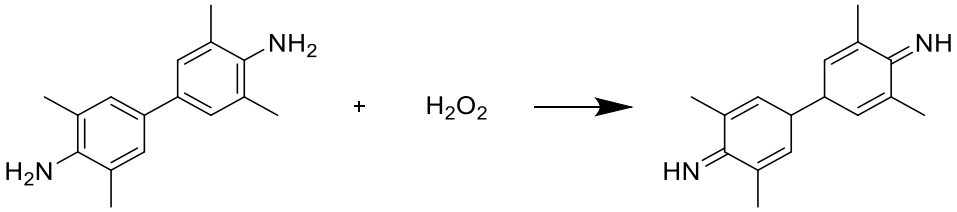

Scheme 6. The oxidation of tetramethylbenzidine by hydrogen peroxide

In a small round-bottom flask we combined 1.95 mL sodium acetate buffer (pH = 4), 0.25 mL 30 mM hydrogen peroxide, 20 mg Flakes/Powders, and 0.25 mL of varying concentrations (0.2 mM, 0.5 mM, 0.8 mM, 1.4 mM, 1.7 mM and 2 mM) of tetramethylbenzidine (TMB) in ethanol. The solution was stirred for 5 minutes during which it changed colour from colourless to blue. The polymer was filtered out and absorbance at 652 nm was measured.

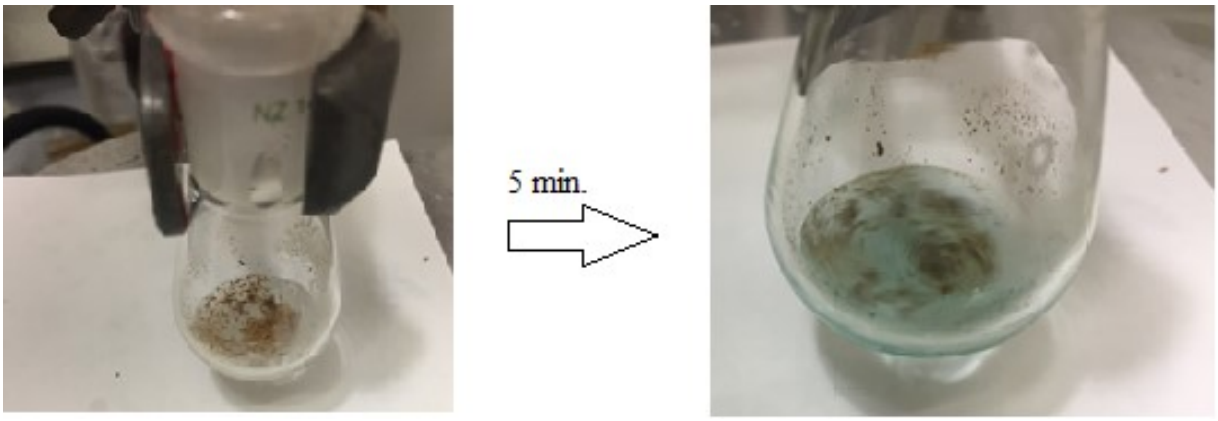

Figure 8 The progress of oxidation of tetramethylbenzidine by H_2O_2 with Flake as an artificial peroxidase

6. Results and Discussion

6.1. Characterisation

The polymer synthetized on copper foil was analysed by thermogravimetric combustion analysis (TGA) under air and nitrogen atmosphere (see *Figure* ***9***). According to this we decided to carbonise our material at 600°C as this temperature corresponds to bigger weight loss under both conditions. On TGA of carbonised polymer (*Figure* ***9***) we can see that the material is thermally stable under nitrogen, but under air there is still a big weight loss between 400°C and 500°C, which is probably due to some parts of the polymer being oxidized during this process. *Table* ***1*** shows yields after the carbonisation, which are lower than expected from TGA probably due to long time of carbonisation, which was 2 hours.

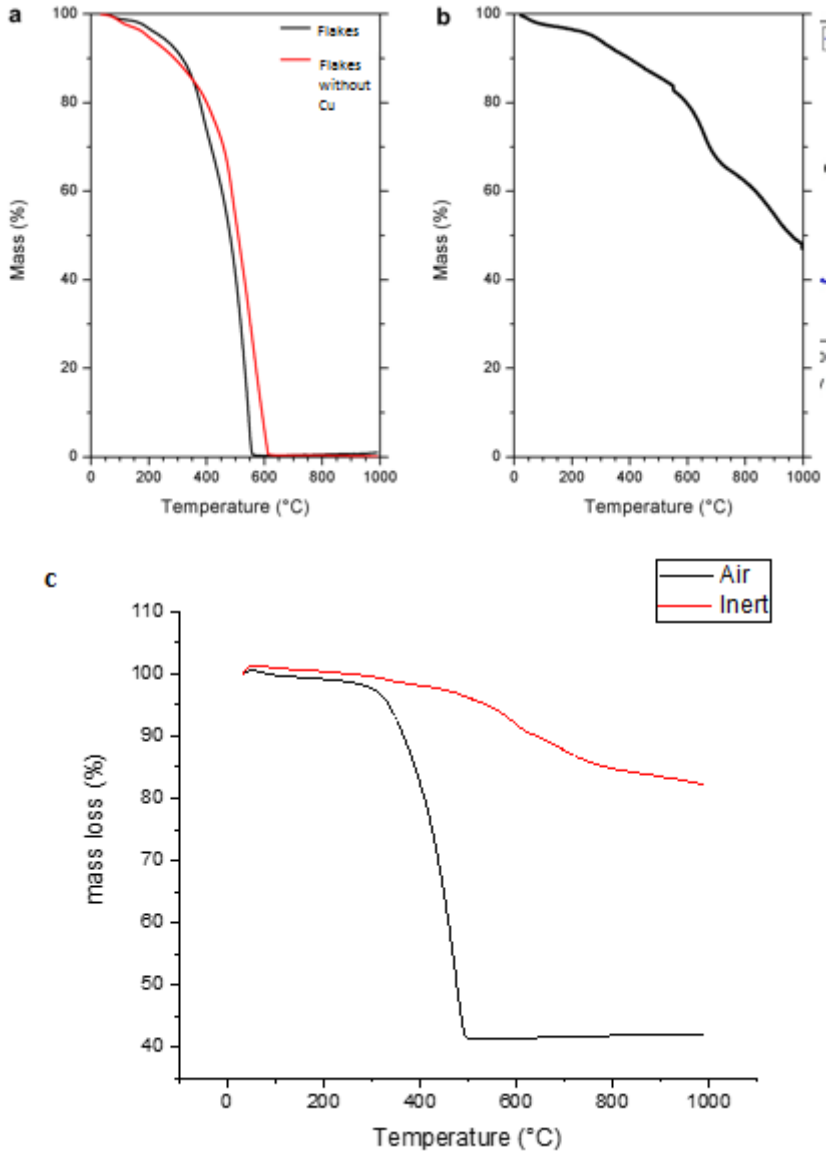

Figure 9 Thermogravimetric analysis for a. Flakes under air, b. Flakes under inert atmosphere, c. Flakes-C600 under inert atmosphere and under air.

Table 1 Yields of polymer after carbonisations

Polymer	Temperature (°C)	Yield (wt.%)
Flakes	600	24.0
Powder	600	45.9
Powder	800	13.8

All polymers were analysed by combustion elemental analyses and ICP-OES measurement in order to determine the copper content. Results of those analyses can be seen in *Table **2***.

Table 2 Ratio of elements determined by combustion elemental analyses and inductively coupled plasma optical emission spectrometry in wt%.

Material	C	N	H	Cu
Theoretical	85.70	11.11	3.17	
Flakes	70.76	9.49	3.88	2.25
Powder	73.64	9.74	3.59	3.08
Flakes-C600	43.62	1.45	4.98	14.30
Powder-C600	56.90	3.46	2.32	6.36
Powder-C800	61.14	2.81	1.73	17.44

As expected the relative amount of copper is larger in the carbonised materials as the organic material is being burnt away and copper stays in the material.

The distribution of sizes of Cu NPs was further investigated via TEM (Transmission electron microscope) imagining. We measured all the Cu nanoparticles on a TEM image of Flakes and Flakes-C600. Then we created a histogram of Cu NP sizes to see how their distribution looks like. The diameters of nanoparticles were bigger in carbonised samples than in non-carbonised. This can be explained by sintering of copper, which is when the copper is forming bigger solid materials under heating lower than the melting point of copper. The sizes of nanoparticles in non-carbonised material were more homogeneous than in carbonised material, which can be explained by a fact that Cu NPs are not homogeneously distributed throughout the material and therefore the size of NPs in carbonised material depends on how many Cu NPs are close together. Mean particle diameter in non-carbonised material was 2 nm and 17 nm in carbonised material.

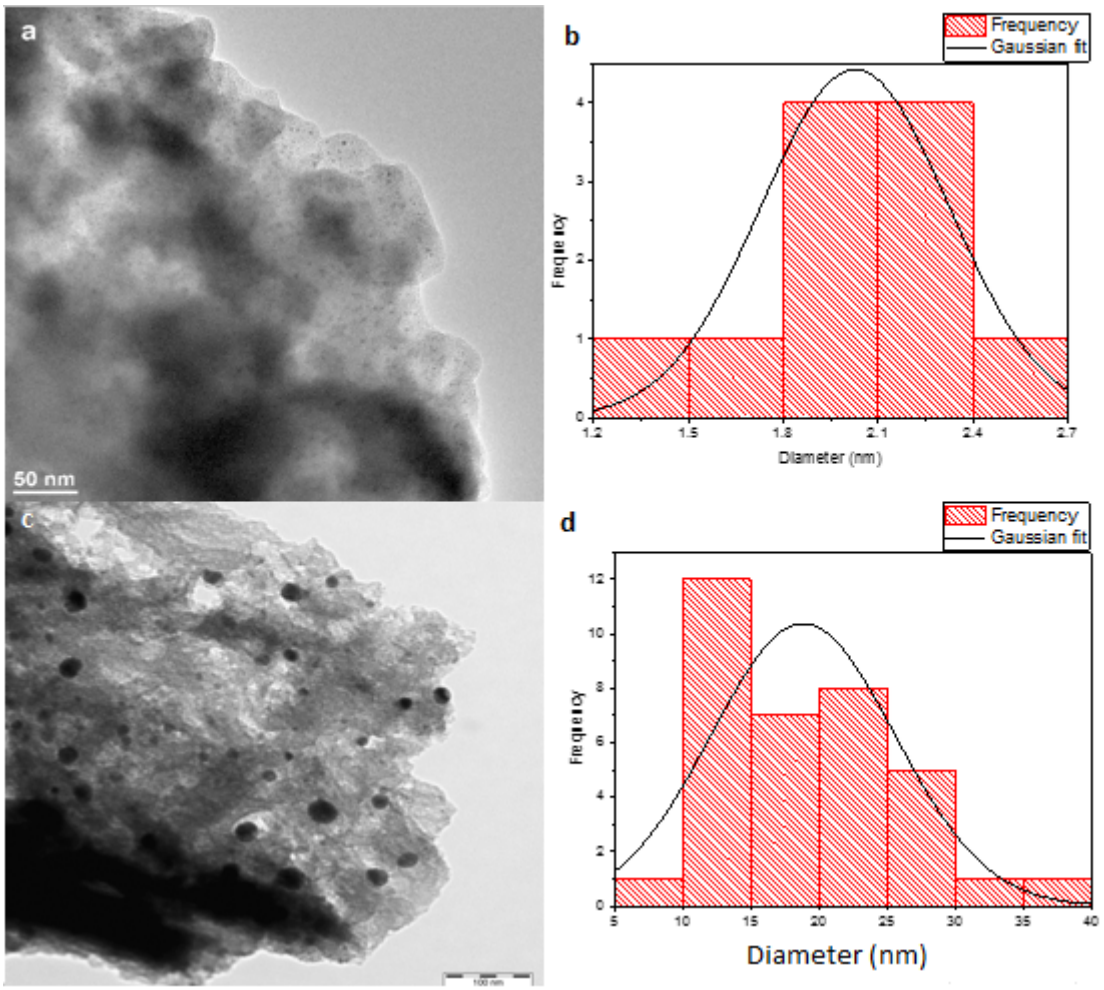

Figure 10 a. transmission electron microscopy picture of Flakes, b. size distribution of particle diameters in Flakes, c. transmission electron microscopy picture of Flakes-C600, d. size distribution of particle diameters in Flakes-C600

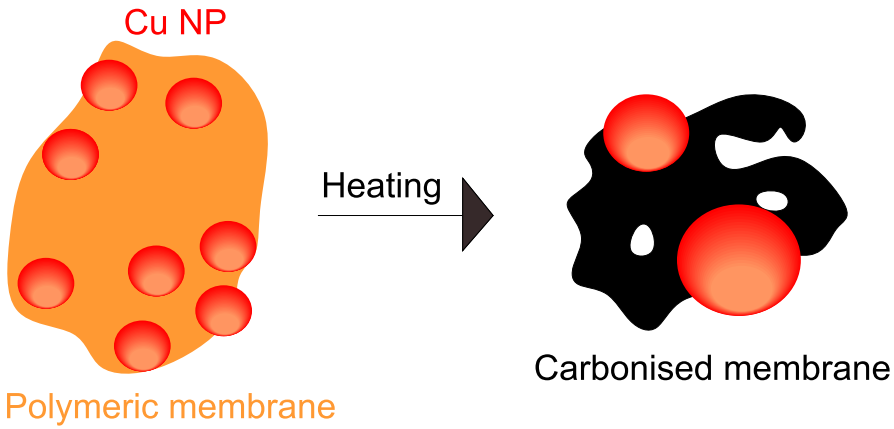

Figure 11. Scheme of creation of bigger copper particles during carbonisation of polymer

The oxidation state of Cu NPs was determined using EPR (Electron Paramagnetic Resonance) and XPS (X-ray Photoelectron Spectroscopy) measurements. In the case of non-carbonised polymer, it was mostly Cu(I), in carbonised polymers mostly Cu (0) was present. XPS did not show Cu(II) species, however some small amount of Cu(II) was visible via EPR measurement.[9, 27]

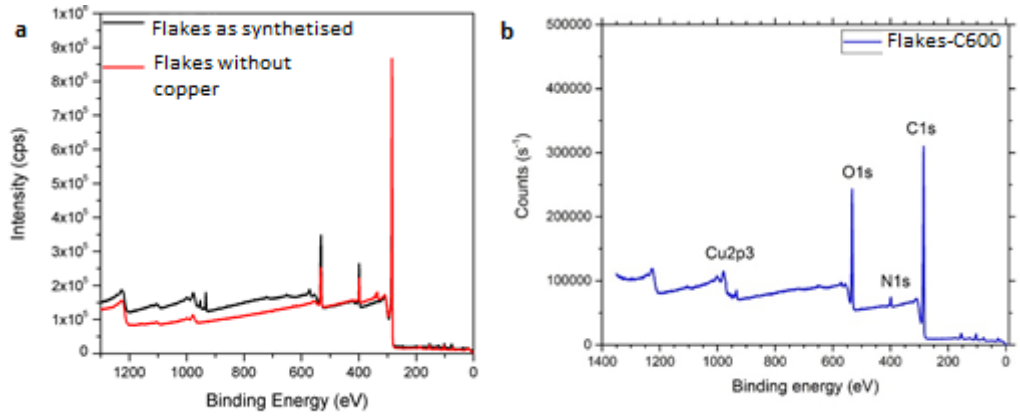

Figure 12 X-ray photoelectron microscopy survey spectra for (a) Flakes with CuNPs and Flakes without CuNPs (b) Flakes with CuNPs carbonised at 600 °C

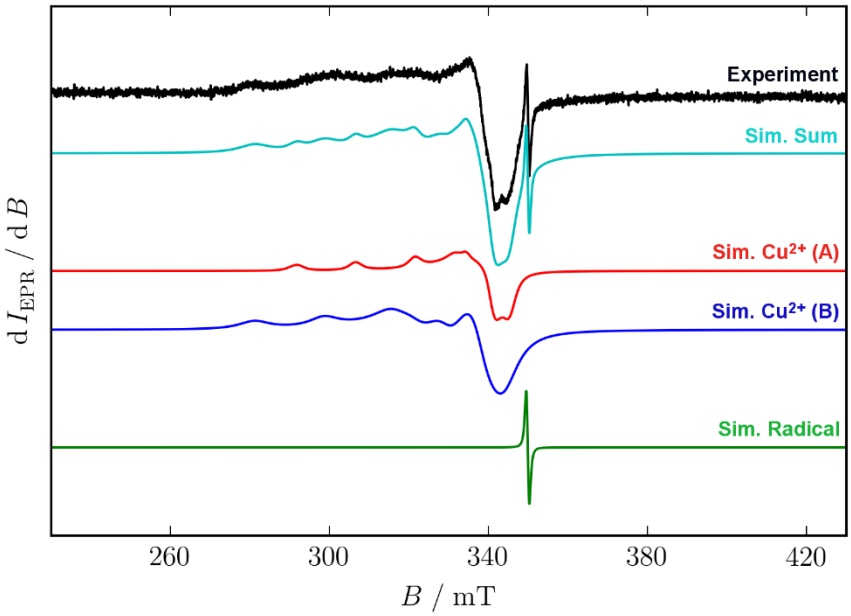

Figure 13. Experimental EPR spectrum (black line) of the Flakes sample. Simulated spectrum ("Sim. Sum", cyan line), which is the sum of individual components coming from two types of paramagnetic copper species: "Sim. Cu2+ (A)" and "Sim. Cu2+ (B)", red and blue l[9]

Surface area was determined by measuring argon or nitrogen sorption isotherms. The isotherms are on *Figure* ***14*** and *Figure* ***15***, and the surface area of all polymers is in *Table* 3. Surface areas of *all polymers*[9, 27] The Powder polymer shows higher surface area than Flakes. After carbonisation the surface area of materials was increased due to creating defects in the structure resulting in more porous structure.

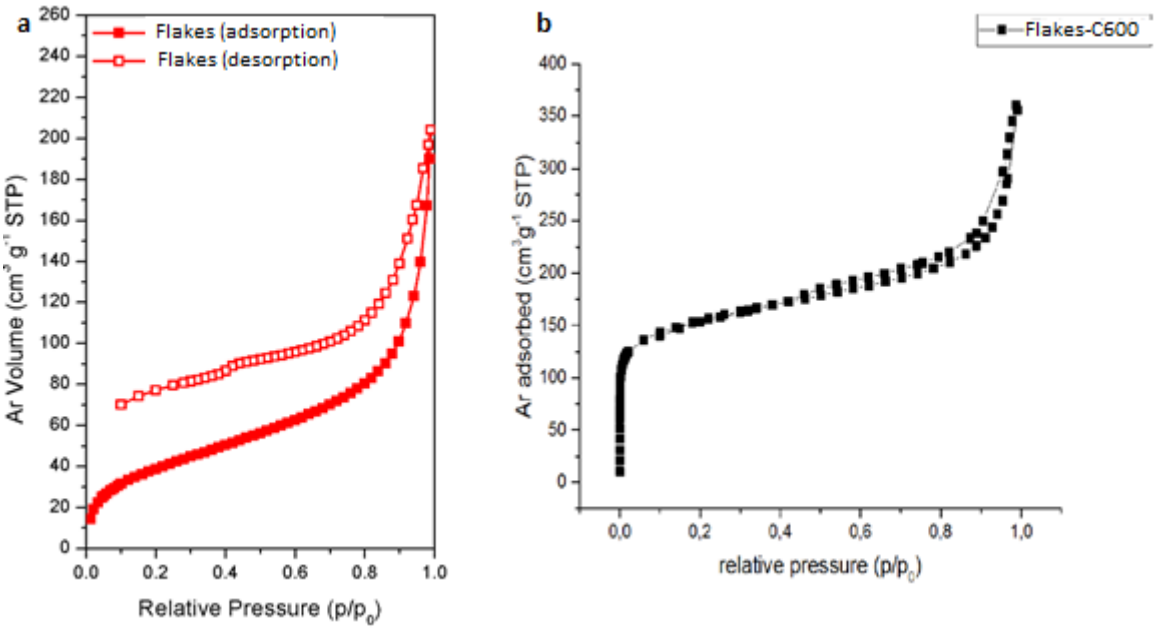

Figure 14. Argon sorption isotherms measured at 88 K for non-carbonised Flakes (a), and Flakes-C600 (b)

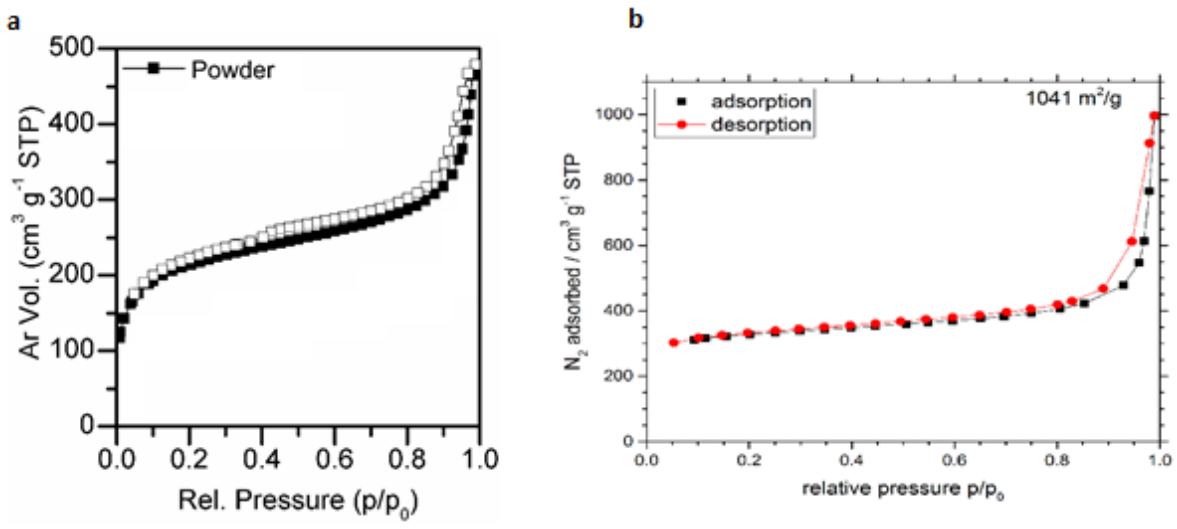

Figure 15. Argon sorption isotherm measured at 88 K for Powder (a), and N_2 sorption isotherm measured at 88K for Powder-C800 (b)

Table 3. Surface areas of all polymers calculated according to Brunauer-Emmett-Teller (BET) model from argon sorption isotherms measured at 88 K, or in case of Powder-C800 nitrogen sorption at 88 K

Polymer	Surface area (m^2/g)
Flakes	124
Powder	659.95
Flakes-C600	477.75
Powder-C800	1041

6.2. ***Catalytic activity***

In order to investigate the catalytic activity of polymer network we performed a set of reactions in different solvents following the reported procedure[8a] and using Flakes grown on copper foil and carbonised at 600 °C. Only in the case of PEG the desired product was observed. Even higher yields were obtained for PEG 400. Therefore, we only tested PEG 400 in catalysis with non-carbonised Flakes, Powder polymer and carbonised Powders. For all carbonised polymers the amount of polymer was chosen according to copper content so that the amount of copper is 10 mol.% of aniline. After the reaction small amount of reaction mixture was taken out and dissolved in acetonitrile, in case of PEG as a solvent we first performed a small extraction to ether, this solution was then analysed by HPLC. The conversion was determined from ratio of surfaces under the curve for each compound in the mixture: the iodobenzene, aniline and diphenylamine. Results of all catalysed reactions are shown in the

Table 4. For comparison, we performed a reaction with pure copper powder which yielded no product after 5 hours.

Table 4. Results of C-N bond formation with different solvents and different materials

Entry	**Solvent**	**Polymer**	**Time [h]**	**Conversion* [%]**
1	Toluene	Flakes C 600	26	0
2	PEG 200	Flakes C 600	5	Less than 1
3	PEG 400	Flakes C 600	5	10
4	Dioxane	Flakes C 600	5	0
5	PEG 400	Powder C 800	5	9
6	PEG 400	Powder C 600	5	11
7	PEG 400	Powder C 600	22	15
8	PEG 400	Powder C 800	22	11
9	PEG 400	Flakes	5	0
10	PEG400	Powder	5	0
11	PEG 400	Flakes	22	0
12	PEG 400	Powder	22	0

*- determined by HPLC

As can be seen from

Table 4 catalytic activity was observed in carbonised materials only with similar results, what indicates that bigger copper particles and higher surface area are more effective for this reaction. After five hours the conversion was not increasing significantly. When comparing our material with other reported catalysts for this reaction it shows a lot smaller catalytic activity, and even though it is noble metal free and heterogeneous other catalysts can be preferred.

6.3 Peroxidase-like mimetics

To test the peroxidase activity of our polymer we performed a TMB oxidation reaction, the formation of blue charge transfer complex was clearly visible and further confirmed by measuring absorbance at 652 nm. To determine steady-state kinetic parameters we performed reactions with varying concentrations of TMB, keeping the concentration of H_2O_2 constant and using the same amount of polymer.

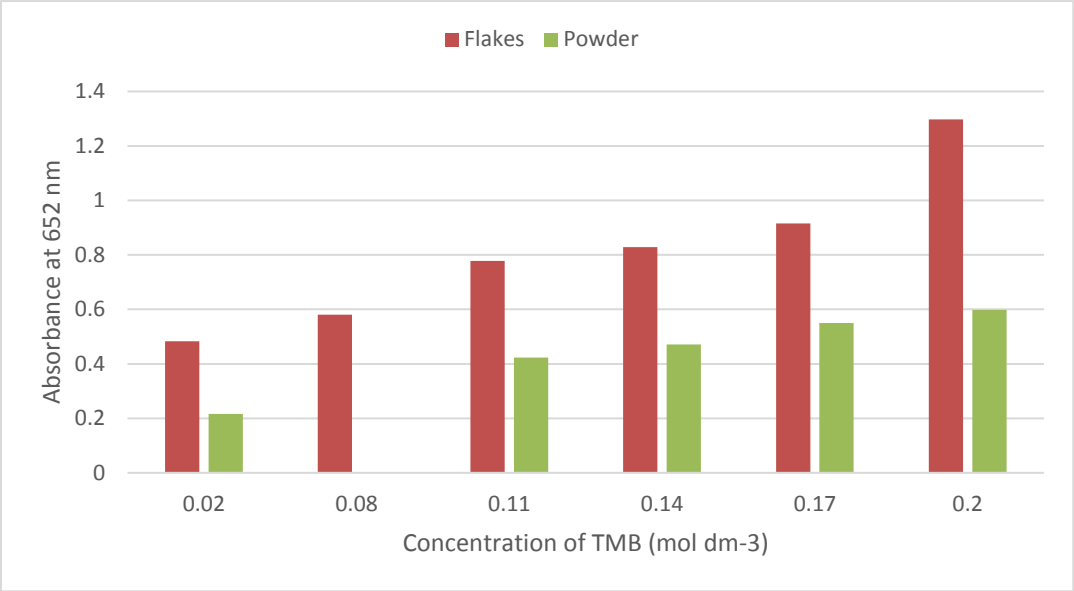

Figure 16. Measured absorbancies at 652 nm with different concentrations of tetramethylbenzidine. Red bars are for Flakes polymer and green for Powder polymer.

To determine the concentration of formed charge transfer complex we measured a single wavelength absorbance at 652 nm and used the Lambert-Beers law, the value of molar extinction coefficient used is 39 000 $M^{-1}cm^{-1}$.[28] We calculated the rate of each reaction and plotted a graph of rate of a reaction over a concentration of a substrate. The rate of the reaction was increasing with the concentration of a substrate as expected. The resulting graphs for Flakes and Powder polymers are on *Figure 17*. To determine the maximum rate of reaction and Michaelis-Menten constant we used Lineweaver-Burke linearization of the Michaelis-Menten kinetics.

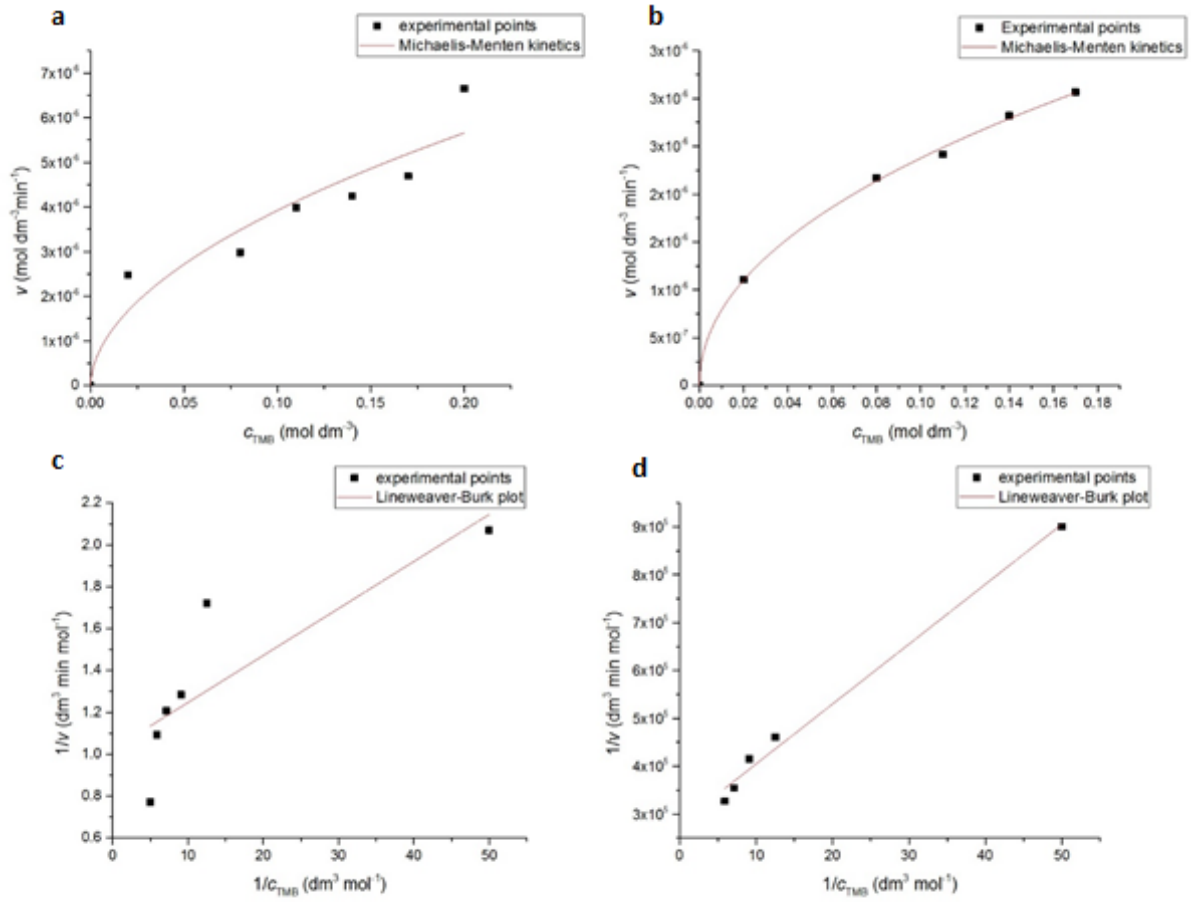

Figure 17 Plots of steady-state kinetic calculations using the Michaelis-Menten model for Flakes (a) and Powder (b), and Lineweaver-Burk models for Flakes (c) and for Powder (d)

The calculated value of Michaelis-Menten constant (K_M) was 0.045 mol dm^{-3} for Powder polymer and 0.022 mol dm^{-3} for Flakes polymer. The value of K_M is an indication of enzyme affinity to a substrate, the smaller the value the bigger the affinity. K_M value of our polymers is higher than the value of horseradish peroxidase and other artificial enzymes, see **Chyba! Nenašiel sa žiaden zdroj odkazov.**. This indicates, that our polymers have smaller binding affinity to the substrate. Values of maximum initial rate of reaction are 0.97 µmol dm^{-3}min^{-1} for Flakes and 0.36 µmol dm^{-3}min^{-1} for Powder polymer.

Table 5. Comparison of Michaelis-Menten constants for tetramethylbenzidine as a substrate of different artificial enzymes and naturally occurring horseradish peroxidase

Catalyst	K_M (mM)	V_{MAX} (10^{-8}Ms^{-1})	Reference
Pt NTs	1.47	-	[29]
Pt-MoO_3	0.106	4.3	[30]
Pd	0.1098	5.82	[31]
Pd-Ir	0.13	6.50	[32]
Graphene/Au-NP hybrids	0.29	5.6	[33]
Citrate-Capped PtNPs	0.1206	6.51	[34]
GOCNT-Pt	0.075	0.302	[35]
MIL-53(Fe)	1.08	8.78	[36]
Hemin@MOF	0.068	6.07	[37]
CuNPs@C	1.65	12.05	[38]
Cu^{2+} – covalent triazine framework	0.057	62.1	[14]
HRP	0.43	10	[39]
Flakes	22	0.00016	This work
Powder	45	0.00006	This work

Further we performed a TMB oxidation reaction with carbonised polymers, which showed smaller peroxidase-like activity, the results of this can be seen in *Table **6***. The activity of carbonised material is lower than that of non-carbonised indicating that smaller particles have better enzyme-like properties. This can be caused by bigger accessible surface area of copper, meaning more active sites. Further the activity of Flakes is more than twice higher than activity of Powder, this can also be explained by the shape of copper present as the Powder polymer does not contain nanoparticles of copper.

Table 6. Reaction rates for tetramethylbenzidine oxidation with different polymers

Polymer	v (μmol dm^{-3} min^{-1})[a]
Flakes	5.33
Powder	2.08
Flakes -C600	3.86
Powder-C600	1.52
Powder-C800	0.90

[a] reaction conditions: 0,78 mL NaAc buffer, 0,1 mL 30mM H_2O_2, 0,1 mL 2mM TMB, 20 mg of polymer, RT

7. Materials and Methods

7.1 Materials

All chemicals and solvents were used as received without further purification. All reactions were done under argon atmosphere on a Schlenk line. All solvents used for preparation of polymer were purchased from VWR and were anhydrous, except for pyridine. Copper foil was purchased from Metall-Ehrnsberger (Teublitz, Germany), its area was 450 cm^2 and was cut to smaller pieces with conventional scissors. Copper (I) chloride was purchased from Across Organics. Aniline was purchased from VWR. Iodobenzene and PEG were purchased from ABCR. Carbonisation of polymers was done in a tubular furnace under nitrogen atmosphere.

7.2 Methods

X-ray photoelectron microscopy (XPS) spectra were recorded on an AXIS ULTRA (Kratos Analytical Ultra, England). Mono-Al $K_{\alpha 1,2}$ source was used with a rated input of the x-ray tube of 300 W at 20 mA. The analyser had a pass energy of 160 eV (overview spectra) and 20 eV (high resolution spectra). Low energy electron source in contact with a magnetic immersion lens was used for charge compensation.

Transmission electron microscopy (TEM) was done using Titan 80-300 instrument (FEI) with an imaging-side spherical aberration corrector operating at an accelerating voltage of 80 kV under Scherzer conditions and with a spherical aberration value of 20 μm. Images were recorded on a CCD (charge-coupled device) with an exposure time one second per frame and an interval of two seconds between the frames at a constant electron dose rate of ~10^7 electrons $nm^{-2}s^{-1}$.

Inductively coupled plasma optical emission spectrometry (ICP-OES) measurements were carried on a SPECTRO ARCOS optical emission spectrometer (SPECTRO Analytical instruments, Kleve, Germany). This instrument features a Paschen-Runge spectrometer mount; the wavelength range between 130 and 770 nm can be analysed simultaneously. An air-cooled ICP-generator, based on free-running 27.12 MHz system is installed. Cyclonic spray chamber and a modified light nebulizer was used for sample introduction. The following ICP operating parameters were used: generator power 1 450 W, coolant flow 13 L/min, auxiliary flow 0.89 L/min, nebulizer flow 0.75 L/min, sample aspiration rate 2 mL/min. Commercially available multielement standard solutions (Analytika, Czech Republic) were used for calibration. The concentrations of calibrated elements were 0, 0.2, 1.0, 5.0, 10.0 and 20.0 mg/L. All measurements were performed in 4 % HNO_3 as a matrix. Sample preparation: the solid samples were weighted on microanalytical balance (aprox. 5 mg) and combusted by Schöniger method. After combustion, the closed Erlenmayer flask was treated in ultrasonic bath for several minutes. After absorption of combustion products (at least 2 hours) 50 μL of 1000 mg/L standard solution were added. The liquid mixture was transferred from glass flask in a plastic bottle. The flask was rinsed carefully with demineralized water which was added to the plastic bottle. The concentration of HNO_3 was adjusted to 4%. The demineralized water was added to plastic bottle to achieve the final

volume 25 mL. After mixing the solution was filtered and introduced to the spectrometer system.

Argon (Ar) sorption measurements were performed using a Micromeritics ASAP 2020 and the isotherm was measured at 88 K. The surface area was calculated in the relative pressure range of 0.05 – 0.35. The samples were degassed at 90°C before analysis.

Nitrogen (N_2) sorption measurements were performed using a Micrometrics ASAP 2020 and Quadrasorb SI from Quantachrome Instruments and the isotherm was measured at 77 K. The surface area was calculated in the relative pressure range of 0.05 – 0.35. The samples were degassed at 90°C before analysis.

Thermogravimetric analysis (TGA) measurements were carried out under air and nitrogen on a Mettler Toledo TGA 1 Stare thermal instrument with a heating rate of 10 K min^{-1} and a gas flow of 20 mL min^{-1} in a 70 μL aluminium oxide crucible.

8. Conclusion

We prepared and characterised triazine-based polymeric materials with embedded CuNPs obtained from a facile one-pot reaction; Flakes, Flakes-C600, Powder, and Powder-C800, as heterogeneous catalysts in two principle morphologies. Membranes of the material were obtained from an on-catalysts synthesis using commercially available copper foil and a bulk polymer powder was obtained via Glaser coupling, using Cu(I) salt as a catalyst. We tuned the porosity and the CuNPs sizes of membranes and powders via carbonisation at 600 °C and 800 °C. Membranes contained copper nanoparticles with mean particle diameters of 2 nm. Carbonisation led via sintering to the formation of larger CuNPs with mean diameters of 17 nm. Furthermore, thermal tempering introduced large transport pores into the structures of membranes and powders leading up to a 3-fold increase in guest-accessible surface area.

We have used the prepared materials as heterogeneous catalysts for a reaction of iodobenzene with aniline in presence of a base, which yielded diphenylamine. We used membrane and powder morphologies of our polymers both in their carbonised and non-carbonised forms. To find the best conditions, a variety of experiments with varying reaction times, solvents, and temperatures was performed using the best-performing system – a flake-like polymer carbonised at 600°C – as the catalyst. These experiments showed, that the use of PEG 400 as solvent at 95° C works best. We used membrane and powder morphologies of our polymers both in their carbonised and non-carbonised forms. The total conversion for Flakes and Powder polymers were similarly low, with a maximum of 15% conversion (after 22h) for Powder carbonised at 600 °C. Non-carbonised polymers did not show any activity at all. Since a mix of Cu(0) and Cu(I) species can be found in both carbonised and non-carbonised samples, these results indicate that the larger accessible surface areas and larger CuNPs of carbonised samples enhance catalytic activity, in particular since the reaction medium (PEG 400) has a good chance to completely “wet” all accessible surfaces. In this study we showed that metallic nanoparticles created ab initio exhibit catalytic activity, but this activity is lot smaller than the activity of other reported catalysts, in particular noble-metal containing catalysts and homogeneous catalysts.

Further, we used the polymeric membrane with embedded Cu NPs and powder like polymer containing copper as an artificial peroxidase mimic. The peroxidase-like activity was tested in the oxidation of tetramethylbenzidine. Our materials showed enzymatic activity, however, inversely to the C-N formation study with non-carbonised samples outperforming carbonised ones. In terms of morphology, Flakes showed better catalytic activity than bulk Powders. Here, we assume that the non-polar surface areas of our materials confer no advantage in terms of activity, since the reaction medium (polar acetate buffer) most likely does not penetrate the microporous channels to a significant extent. Therefore, the small Cu NPs at the surface of the polymer Flakes yield themselves better for enzyme-mimetics. When comparing our material to other reported artificial peroxidases, our materials show an overall higher K_M value indicating smaller bonding affinity to the substrate.

9. References

[1] P. Anastas, J. Warner,**1998.** Green chemistry: Theory and Practice; Oxford University Press

[2] M. Negwer, **1994**. Organic-chemical drugs and their synthesis (survey) 7th ed; Akademie Verlag GmbH

[3] J. H. Montgomery, **1993**. agrochemicals Desk Reference> enviromental Data; Montgomery, J.H

[4] R. O. H. Loutfy, C. K.; Kazmaier, P. M, *Sci. Eng.* **1983**, *27*, 5-9.

[5] J. Louie, J. F. Hartwig, A. J. Fry, *Journal of the American Chemical Society* **1997**, *119*, 11695-11696.

[6] a) P. Paul, R. J. Butcher, S. Bhattacharya, *Inorganica Chimica Acta* **2015**, *425*, 67-75; b) W. C. Shakespeare, *Tetrahedron Letters* **1999**, *40*, 2035-2038; c) J. F. Hartwig, *Synlett* **1997**, *1997*, 329-340; d) J. Rouden, A. Bernard, M.-C. Lasne, *Tetrahedron Letters* **1999**, *40*, 8109-8112.

[7] a) D. M. T. Chan, K. L. Monaco, R.-P. Wang, M. P. Winters, *Tetrahedron Letters* **1998**, *39*, 2933-2936; b) P. Y. S. Lam, C. G. Clark, S. Saubern, J. Adams, M. P. Winters, D. M. T. Chan, A. Combs, *Tetrahedron Letters* **1998**, *39*, 2941-2944; c) S. M. Islam, S. Mondal, P. Mondal, A. S. Roy, K. Tuhina, N. Salam, M. Mobarak, *Journal of Organometallic Chemistry* **2012**, *696*, 4264-4274; d) A. Tirsoaga, B. Cojocaru, C. Teodorescu, F. Vasiliu, M. N. Grecu, D. Ghica, V. I. Parvulescu, H. Garcia, *Journal of Catalysis* **2016**, *341*, 205-220; e) J. C. A. Artis Klapars, Xiaohua Huang, and, and Stephen L. Buchwald, *Journal of the American Chemical Society* **2001**, *123*, 7727-7729.

[8] a) M. Kidwai, Mishra, N. K., Bhardwaj, S., Jahan, A., Kumar, A. and Mozumdar, S., *ChemCatChem* **2010**, *2*, 1312-1317; b) R. K. Borah, P. K. Raul, A. Mahanta, A. Shchukarev, J.-P. Mikkola, A. J. Thakur, *Synlett* **2017**, *28*, 1177-1182.

[9] D. Schwarz, Y. Noda, J. Klouda, K. Schwarzová-Pecková, J. Tarábek, J. Rybáček, J. Janoušek, F. Simon, M. V. Opanasenko, J. Čejka, A. Acharjya, J. Schmidt, S. Selve, V. Reiter-Scherer, N. Severin, J. P. Rabe, P. Ecorchard, J. He, M. Polozij, P. Nachtigall, M. J. Bojdys, *Advanced Materials* **2017**, 1703399.

[10] J. Riordan, *Annals of Clinical & Laboratory Science* **1977**, *7*, 119-129.

[11] M. Raynal, P. Ballester, A. Vidal-Ferran, P. W. N. M. van Leeuwen, *Chem. Soc. Rev.* **2014**, *43*, 1734-1787.

[12] a) D. Desbois *Coordination Chemistry Reviews* **2012**, *256*, 897-937; b) P. J. Deuss, G. Popa, A. M. Z. Slawin, W. Laan, P. C. J. Kamer, *ChemCatChem* **2013**, *5*, 1184-1191; c) H. Derakhshankhah, A. A. Saboury, A. Divsalar, H. Mansouri-Torshizi, I. Bamery, D. Ajloo, A. A. Moosavi-Movahedi, R. Hosseinzadeh, M. R. Ganjali, H. Ilkhani, H. R. Khavasi, *Journal of the Iranian Chemical Society* **2014**, *11*, 1381-1390.

[13] a) Y. Zhao Yiqun Zheng Rongmei Kong Lian Xia Fengli Qua, *Biosensors and Bioelectronics* **2016**, *75*, 383-388; b) F. W. Krainer, A. Glieder, *Applied microbiology and biotechnology* **2015**, *99*, 1611-1625; c) H. Cheng, L. Zhang, J. He, W. Guo, Z. Zhou, X. Zhang, S. Nie, H. Wei, *Analytical Chemistry* **2016**, *88*, 5489-5497.

[14] Y. Xiong, Y. Qin, L. Su, F. Ye, *Chemistry - A European Journal* **2017**, *23*, 11037-11045.

[15] M. M. Heravi, Z. Kheilkordi, V. Zadsirjan, M. Heydari, M. Malmir, *Journal of Organometallic Chemistry* **2018**, *861*, 17-104.

[16] L. Chen, G.-A. Yu, F. Li, X. Zhu, B. Zhang, R. Guo, X. Li, Q. Yang, S. Jin, C. Liu, S.-H. Liu, *Journal of Organometallic Chemistry* **2010**, *695*, 1768-1775.

[17] A. R. Hajipour, F. Dordahan, F. Rafiee, *Applied Organometallic Chemistry* **2013**, *27*, 704-706.

[18] N. M. Patil, S. P. Gupte, R. V. Chaudhari, *Applied Catalysis A: General* **2010**, *372*, 73-81.

[19] K. A. Johnson, R. S. Goody, *Biochemistry* **2011**, *50*, 8264-8269.

[20] O. Kirk, T. V. Borchet, C. C. Fuglsang, *Current Opinion in Biotechnology* **2002**, *13*, 345-351.

[21] R. Ragg, M. N. Tahir, W. Tremel, *European Journal of Inorganic Chemistry* **2016**, *2016*, 1906-1915.

[22] H. Wei, E. Wang.; Anal. Chem. **2008**, 80, 2250-2254

[23] L. Su, Y. Xiong, H. Yang, P. Zhang, F. Ye, *J. Mater. Chem. B* **2016**, *4*, 128-134.

[24] a) J. Liu, P. Ruffieux, X. Feng, K. Mullen, R. Fasel, *Chemical Communications* **2014**, *50*, 11200-11203; b) F. Xiang, Y. Lu, C. Li, X. Song, X. Liu, Z. Wang, J. Liu, M. Dong, L. Wang, *Chemistry – A European Journal* **2015**, *21*, 12978-12983.
[25] J. Eichhorn, W. M. Heckl, M. Lackinger, *Chemical Communications* **2013**, *49*, 2900-2902.
[26] K. S. Sindhu, G. Anilkumar, *RSC Advances* **2014**, *4*, 27867-27887.
[27] D. Schwarz, *Advanced Functional Materials* **2018**.
[28] L. A. Marquez, H. B. Dunford, *Biochemistry* **1997**, *36*, 9349-9355.
[29] Q. Shi, Y. Song, C. Zhu, H. Yang, D. Du, Y. Lin, *ACS Applied Materials & Interfaces* **2015**, *7*, 24288-24295.
[30] Y. Wang, X. Zhang, Z. Luo, X. Huang, C. Tan, H. Li, B. Zheng, B. Li, Y. Huang, J. Yang, Y. Zong, Y. Ying, H. Zhang, *Nanoscale* **2014**, *6*, 12340-12344.
[31] J. Wei, X. Chen, S. Shi, S. Mo, N. Zheng, *Nanoscale* **2015**, *7*, 19018-19026.
[32] X. Xia, J. Zhang, N. Lu, M. J. Kim, K. Ghale, Y. Xu, E. McKenzie, J. Liu, H. Ye, *ACS Nano* **2015**, *9*, 9994-10004.
[33] M. Liu, H. Zhao, S. Chen, H. Yu, X. Quan, *ACS Nano* **2012**, *6*, 3142-3151.
[34] G.-W. Wu, S.-B. He, H.-P. Peng, H.-H. Deng, A.-L. Liu, X.-H. Lin, X.-H. Xia, W. Chen, *Analytical Chemistry* **2014**, *86*, 10955-10960.
[35] H. Wang, S. Li, Y. Si, N. Zhang, Z. Sun, H. Wu, Y. Lin, *Nanoscale* **2014**, *6*, 8107-8116.
[36] L. Ai, L. Li, C. Zhang, J. Fu, J. Jiang, *Chemistry – A European Journal* **2013**, *19*, 15105-15108.
[37] F.-X. Qin, S.-Y. Jia, F.-F. Wang, S.-H. Wu, J. Song, Y. Liu, *Catalysis Science & Technology* **2013**, *3*, 2761-2768.
[38] H. Tan, C. Ma, L. Gao, Q. Li, Y. Song, F. Xu, T. Wang, L. Wang, *Chemistry – A European Journal* **2014**, *20*, 16377-16383.
[39] L. Gao, J. Zhuang, L. Nie, J. Zhang, Y. Zhang, N. Gu, T. Wang, J. Feng, D. Yang, S. Perrett, X. Yan, *Nature nanotechnology* **2007**, *2*, 577-583.